UDC 544.643-621.357

R.D. Apostolova, R.P. Peskov

INCREASING THE EFFICIENCY OF THIN-LAYER Co-DOPED $LiMn_2O_4$–CARBON NANOTUBES ELECTRODES FOR THE USE IN Li-ION BATTERIES

Ukrainian State University of Chemical Technology, Dnipro, Ukraine

The analysis of galvanostatic curves, cyclic voltammograms and impedance parameters was performed in order to determine and interpret the key factors responsible for the decrease of the discharge characteristics of thin-layer composite Co-doped $LiMn_2O_4$ spinel–carbon nanotubes (CNT) electrodes in redox reaction with lithium during continuous cycling at low temperature and high charge-discharge rate. The comparison of galvanostatic curves and cyclic voltammograms obtained by using three-electrode and two-electrode experimental cells was carried out; the impedance spectra as functions of temperature and charge-discharge rate were considered too. This allowed following the evolution of degenerative electrode processes without the usage of research techniques which are complicated and not accessible enough. The charge transfer through the solid-electrolyte interface between solid-electrolyte film/spinel composite, complicated by diffusion of Li^+ ions in composite bulk, plays a key role in decreasing the discharge characteristics of Co-doped $LiMn_2O_4$ spinel composition with CNT at low temperatures and continuous cycling. It was established that the processes of anodic decomposition of the electrolyte starting at 4.13 V vs. Li/Li^+-electrode and low conductivity of electrolyte EC, DMC, 1 mol L^{-1} $LiClO_4$ at low temperatures (258 K) have a negative influence on the effective electrochemical performance of accumulator system $LiCo_{0.04}Mn_{1.96}O_4$, CNT-electrodes/electrolyte/Li. A further optimization of the electrolyte with the use of some efficient additions to the developed spinel composite can be a possible way to improve the electrode performance. A decrease in the conductivity of $LiMn_2O_4$ spinel results in a decrease in the capacity at low temperature (258 K). The modification of the spinel composite seems to be very promising to suppress its low-temperature phase transitions. The elimination of the established reasons for decreasing the capacity will facilitate the realization of new promising $LiCo_{0.04}Mn_{1.96}O_4$–CNT electrode material in lithium ion accumulators.

Keywords: lithium-ion accumulator, Co-doped $LiMn_2O_4$ spinel, carbon nanotubes, capacity, galvanostatic curves, cyclic voltammograms, impedance spectra.

Introduction

$LiMn_2O_4$ spinel can be used in lithium-ion batteries due to a number of its advantages (low price and non-toxicity). However, it also has a number of shortcomings. It is, inter alia, a low rate of discharge caused by the low spinel conductivity and the decrease of discharge capacity of $LiMn_2O_4$ in lithium-ion batteries during long cycling, particularly at low temperatures.

The effective electrochemical performance of $LiMn_2O_4$ spinel in redox reaction with lithium is dependent on the conductive filler. In our previous investigations, we showed the improvement of the capacity, rate characteristics of $LiMn_2O_4$ spinel under the influence of carbon nanotubes (CNT) used as the filler. A high coulomb efficiency of $LiMn_2O_4$ spinel performance in redox reaction with lithium was observed when CNT was used to increase the conductivity [1]. The effective exchange current of $LiMn_2O_4$ spinel electrode (i_0) increases from the order of 10^{-7} to 10^{-4} $A \cdot cm^{-2}$ in the presence of CNT. The effective exchange current of $LiMn_2O_4$ spinel–CNT composite electrode at the potentials corresponding to maximum activity in deintercalation processes is 2.2–3.0 times higher than the exchange current of the composite with natural micrometer graphite as the filler. The discharge capacity of $LiMn_2O_4$–CNT electrodes in the first cycles reaches 117–119 $mA \cdot h \cdot g^{-1}$ at the rate of 1 C (98–100 $mA \cdot h \cdot g^{-1}$ at 22.4 C) and cycling can be continued at high discharge rate during

more than 500 charge-discharge cycles at 290–298 K [1].

The improvement of discharge characteristics of $LiMn_2O_4$–CNT compositions was achieved by Co-doping of $LiMn_2O_4$ [2]. The high temperature synthesis was used to produce skin-deep Co-doped $LiMn_2O_4$ spinel. The surface Co-doping promotes an increase in the electroconductivity of pressed $LiMn_2O_4$ spinel at the temperatures of 293 and 323 K. The advantage of Co-doped $LiMn_2O_4$ composition with CNT over the composition without Co is an increase in cyclic efficiency and the rate of Li^+-intercalation/deintercalation in thin-layer electrodes. The discharge capacity of Co-doped $LiMn_2O_4$–CNT thin-layer electrodes at 40 C (1 C=118 $mA{\cdot}h{\cdot}g^{-1}$) and the temperatures of 293–298 K reaches 75% (90 $mA{\cdot}h{\cdot}g^{-1}$) in terms of the start capacity obtained in the first cycle [2]. The capacity of un-doped $LiMn_2O_4$–CNT electrodes equals to 80 $mA{\cdot}h{\cdot}g^{-1}$ at 20 C and ambient temperature. A satisfactory cycling performance of Co-doped $LiMn_2O_4$–CNT electrodes was obtained at lower temperatures and 1 C. At the same time, their high discharge characteristics at low temperatures (273 and 258 K) change for the worse when the rate of the electrode processes increased to 10 C.

Earlier, the determination of the causes of a decrease in the discharge capacity of Co-doped $LiMn_2O_4$–CNT electrode in redox reaction with lithium was performed by means of impedance spectroscopy [2].

In this work we made an attempt to analyze the relationships between the features of galvanostatic charge-discharge curves, cycling voltammograms and electrochemical impedance characteristics of thin-layer Co-doped $LiMn_2O_4$–CNT electrodes, particularly, at low temperatures and long cycling. The aim of the work was to establish the causes of a decrease in the discharge capacity of lithium accumulator.

Experimental

Co-doped $LiMn_2O_4$ spinel with chemical formula $LiCo_{0.04}Mn_{1.96}O_4$ was synthesized and used in thin-layer electrodes. The surface Co-doping of $LiMn_2O_4$ spinel was carried out by the thermal treatment of stoichiometric mixture of $LiMn_2O_4$ spinel powder (Merck) and $Co(NO_3)_2{\cdot}6H_2O$ ("pure") (98 and 2 wt.%, respectively) at 650^0C for 2 h in air atmosphere [2]. Thin-layer electrodes were prepared by mechanical embedding of the mixture of Co-doped $LiMn_2O_4$ spinel powder and CNT (90:10 wt.%) in aluminum matrix with dimensions of 1.0×1.0×0.1 cm according to the method described elsewhere [3]. Then the thermal activation (280^0C, 2 h, air atmosphere) was performed. The weight of active spinel component in the electrode was 0.2–0.5 $mg{\cdot}cm^{-2}$; the thickness of active layer was about 0.5–0.8 mm. The electrode does not contain any ballast component of traditional composite electrodes (the so-called binder).

Carbon nanotubes were synthesized by catalytic pyrolysis of ethylene and used as a conductive additive [4]. The outer diameter of nanotubes was about 10–30 nm, the specific surface was 230 $m^2{\cdot}g^{-1}$, the poured density was 25–30 $g{\cdot}dm^{-3}$.

The electrochemical investigations of $LiCo_{0.04}Mn_{1.96}O_4$–CNT electrodes were performed in a sealed three-electrode cell with Li counter electrode, Li/Li^+ reference electrode as well as in a two-electrode cell with Li counter electrode. The cells were filled in argon atmosphere with electrolyte containing ethylene carbonate (EC, Merck), dimethyl carbonate (DMC, Merck), and 1 mol L^{-1} $LiClO_4$ (Iodobrom). The charge-discharge characteristics were recorded using a test bench with computer control and registration. The electrochemical impedance spectra (EIS) and cyclic voltammograms (CV) were obtained using Volta Lab PGZ 301 analytical radiometer. The impedance spectra were recorded at the amplitude of 5–10 mV in the frequency range of 10^{-6} to 10^{-2} Hz at the temperatures of 258 and 296 K. The temperature was determined with a precision of ±0.5 K. Zplot, Zview (Version 2.1 b) software was used to record and analyze the impedance spectra. The parameters of EIS were determined by the analysis of Nyquist plots of the investigated specimens using a model developed in work [5].

Results and discussion

The comparison of the electrochemical parameters obtained by galvanostatic mode and in cyclic voltammetry experiments was performed together with the analysis of EIS parameters of $LiCo_{0.04}Mn_{1.96}O_4$–CNT composite, which possesses a highly stable reversible capacity. The investigations were conducted at room temperature (T_{room}=296 K) and also at a lower temperature (258 K).

Galvanostatic studies on $LiCo_{0.04}Mn_{1.96}O_4$–CNT electrodes in redox reactions with lithium

The galvanostatic studies at room temperature showed the dependence of the discharge profile of thin-layer $LiCo_{0.04}Mn_{1.96}O_4$–CNT electrodes on the discharge rate (Fig. 1). The discharge safe capacity at the 50^{th} cycle equals to 117–119 $mA{\cdot}h{\cdot}g^{-1}$ at a discharge-charge rate of 1 C. The capacity decreases at an increase in the discharge and charge rates from 1 C to 10 C. The variations of the charge-discharge profile with the rate changes were determined in

two-electrode and three-electrode cells for the elucidation of the causes of the discharge capacity drop in the spinel composite and the accumulator on its base. The discharge capacity of $LiCo_{0.04}Mn_{1.96}O_4$–CNT electrodes (with a weight of 0.22 mg·cm^{-2}) reaches 112 mA·h·g^{-1} when $i_{discharge}$=10 C and i_{charge}=1 C (in three-electrode cell, Fig. 2, curves 1–1^I). The difference of the potentials is observed between charge curves 1^I and 2^I (Fig. 2) at an increase in the charge rate. It concerns, to a large degree, that region of the charge curves which in two-phase $LiMn_2O_4$ performance (Eqs. (1) and (2)) is associated with the redox couple at 4.12/4.14 V (site II, Eq. (2)):

$$LiMn_2O_4 \leftrightarrow Li_{0.5}Mn_2O_4 + 0.5Li^+ + 0.5\bar{e}$$
(4.01/4.05 V, site I); (1)

$$Li_{0.5}Mn_2O_4 \leftrightarrow Mn_2O_4 + 0.5Li^+ + 0.5\bar{e}$$
(4.12/4.14 V, site II). (2)

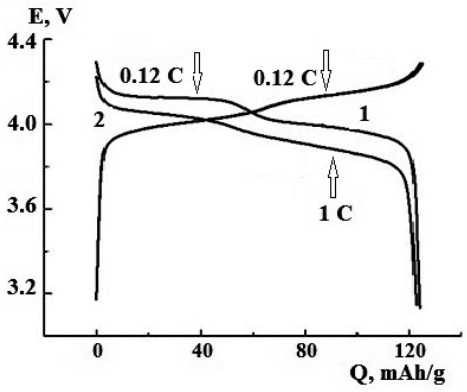

Fig. 1. Charge-discharge characteristics of $LiCo_{0.04}Mn_{1.96}O_4$–CNT electrodes obtained in two-electrode cell at the charge rate of 0.12 C and the discharge rate of 1 C and 0.12 C at the temperature of 296 K

The noticeable growth of charge potential starts at 4.13 V (curve 1^I) and at 4.16 V (curve 2^I) (Fig. 2). This behavior is caused by the side effect of anodic decomposition of the electrolyte. The charge capacity of active electrode material and conjugates decrease with a decrease in the capacity of intercalation of Li^+ ions in following cycle (Fig. 2, curve 2).

The charge-discharge profile of $LiCo_{0.04}Mn_{1.96}O_4$–CNT electrodes obtained in two-electrode cell (Fig. 3) differs from the profile obtained in three-electrode cell (Fig. 2). The difference of charge voltage is observed between curves 1^I and 2^I (Fig. 2) at charge rates of 10 C and 1 C. The difference of the potentials in Fig. 2 when the charge rate increases from 1 to 10 C can be explained in three-electrode cell by increased anodic polarization of composite $LiCo_{0.04}Mn_{1.96}O_4$–CNT electrode (η_{compos}). One should also take into consideration the effect of the electrolyte decomposition in charging (η_{side}).

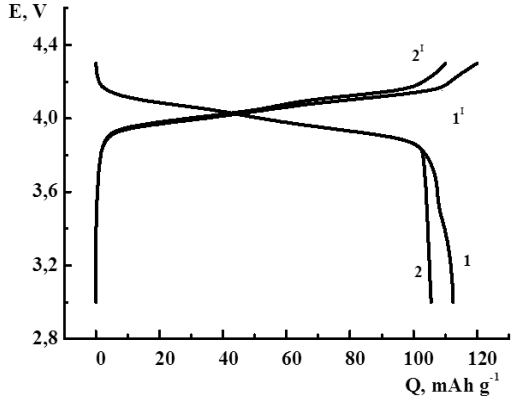

Fig. 2. Charge-discharge characteristics of $LiCo_{0.04}Mn_{1.96}O_4$–CNT electrodes obtained in three-electrode cell at the charge rate of i_1=1 C (curves 1^I) and i_2=10 C (curve 2^I); the discharge rate was 10 C at the temperature was 296 K

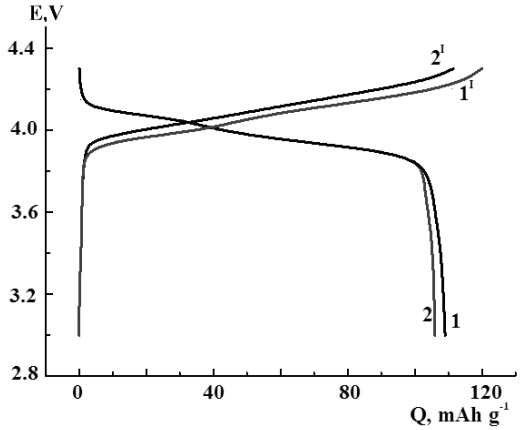

Fig. 3. Charge-discharge characteristics of $LiCo_{0.04}Mn_{1.96}O_4$–CNT electrodes obtained in two-electrode cell at the charge rate of 1 C (curve 1^I) and 10 C (curve 2^I); the discharge rate was 10 C and the temperature was 296 K

Thus, the difference of the total voltage in two-electrode cell can be explained by increased anodic polarization of composite spinel electrode (η_{compos}), polarization of lithium (η_{Li}), voltage drop in electrolyte (iR_{el}) and side effect η_{side} (Fig. 3).

The average effective polarization resistance $R_{compos(galvan)}$, which is determined as dE/di (Fig. 2, where $dE=E_2-E_1$, $di=i_2-i_1$), is equal to 80 ohm·cm^{-2}

if η_{side} is not taken into consideration. The average effective value of the parameters sum ($R_{sum}=R_{compos}+R_{Li}+iR_{el}$) determined from the data of charge curves in Fig. 3 is equal to 190 ohm·cm^{-2}. Thus, the calculated average effective value ($R_{Li}+iR_{el}$) is equal to 110 ohm·cm^{-2}. The results of the analysis can indicate that the decrease of discharge capacity of $LiCo_{0.04}Mn_{1.96}O_4$–CNT/electrolyte/Li system at room temperature and high charge rate occurs not only due to $LiCo_{0.04}Mn_{1.96}O_4$–CNT polarization (η_{compos}). The other constituents (i.e. $\eta_{Li}+iR_{el}$) are essential too. The difference between discharge profiles obtained at the rate of 10 C and 1 C is displayed only at the end of the discharge process and is accompanied by a substantial growth of the charge potentials (at 4.13 and 4.16 V). The value of R_{end} reaches 695 ohm·cm^{-2} at the end of charging. We suppose that the difference between R_{end} and R_{sum} is mainly due to the following R_{side}=505 Ohm·cm^{-2}.

Turning to the results obtained at 296 K, it should be noted that just an insignificant decrease in the discharge capacity of thin-layer $LiCo_{0.04}Mn_{1.96}O_4$–CNT electrodes is observed in redox reaction with lithium (2.0–3.6%) when the intercalation/deintercalation rate increases from 1 C to 10 C at T_{room} 75% of the start capacity is provided by $LiCo_{0.04}Mn_{1.96}O_4$–CNT electrode/Li at the rate of 40 C, the room temperature and charge rate of 1 C.

The role of the rate effect amplifies at the lower temperature is seen from the results of the investigations of $LiCo_{0.04}Mn_{1.96}O_4$–CNT electrodes at the rates of 1 C and 10 C in three-electrode cells (Fig. 4). The anodic polarization of $LiCo_{0.04}Mn_{1.96}O_4$–CNT electrode increased at final charge voltage (E_{end}=4.3 V). The discharge capacity is relatively high at discharge rate of 10 C, the temperature of 258 K and the deintercalation rate of 1 C (Fig. 4, curves 1–1^I in three-electrode cell). However, the discharge profile greatly differs from that at 296 K because of the presence of iR-component. The charge capacity and corresponding discharge capacity decrease at the rate of 10 C (Fig. 4, curves 2^I, and 2).

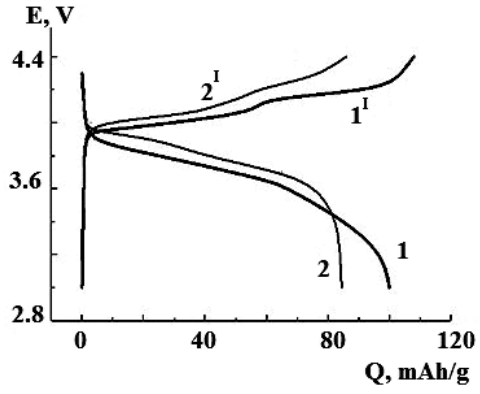

Fig. 4. Charge-discharge characteristics of $LiCo_{0.04}Mn_{1.96}O_4$–CNT electrodes obtained in three-electrode cell at the charge rate of 1 C (curves 1^I) and 10 C (curve 2^I); the discharge rate was 10 C at the temperature was 258 K

A considerable difference is between the charge curves 1^I–2^I at the rates of 1 C and 10 C and discharge curves at 10 C in two-electrode and in three-electrode cells, respectively, at the temperature of 258 K (Fig. 5). The capacity can increase if the charge voltage grows (Fig. 5). The capacity of composite grows with an increase in the charge voltage to 4.5 and 4.6 V and discharge curve is transformed into much typical profile, particularly, in site II. It assumes a high potential possibility of effective composite performance at a low temperature in the electrolyte with wider window of the electrochemical stability than electrolyte used in the work. However, it is known that $Li_2Mn_2O_4$ is an insulator with poor kinetics of lithium exchange that is formed on $LiMn_2O_4$ surface at 4.5 V in an electrolyte containing EC, DMC, 1 mol L^{-1} $LiPF_6$ [6].

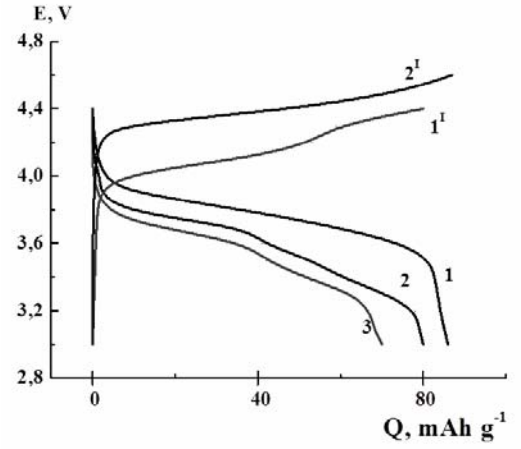

Fig. 5. Charge-discharge characteristics of $LiCo_{0.04}Mn_{1.96}O_4$–CNT electrodes obtained at the charge and the discharge rate of 10 C at the temperature of 258 K in three-electrode cell (curves 1, 1^I) and in two-electrode cell (curves 2, 3, 2^I). E_{end}=4.4 V (curve 1^I) or E_{end}=4.6 V (curve 2^I). The curve 3 was obtained after charging at 10 C and E_{end}=4.5 V

The distinction between charge-discharge capacity of $LiCo_{0.04}Mn_{1.96}O_4$–CNT electrodes obtained in three-electrode cell (Fig. 6 curves 1, 1^I) and in two-electrode cell (Fig. 6, curves 2, 2^I) at the charge rate of 1 C and discharge rate of 10 C at the temperature of 258 K is insignificant. However, the discharge curve profiles are highly different. The distinctions increase at long cycling of

$LiCo_{0.04}Mn_{1.96}O_4$–CNT electrodes. The loss of capacity at the 250th cycle reaches 19% because of increased ($\eta_{Li}+iR_{electrolyte}$) component.

The difference of discharge capacities of $LiCo_{0.04}Mn_{1.96}O_4$–CNT electrodes observed in three-electrode cell and in two-electrode cell at the charging at 1 C and 10 C at room temperature (296 K) is equal to 1.0% when the discharge rate is 10 C. At lower temperature (258 K), the difference is 4.5% at charging at 1 C and is 19.0 % at charging at 10 C when the discharge rate is 10 C.

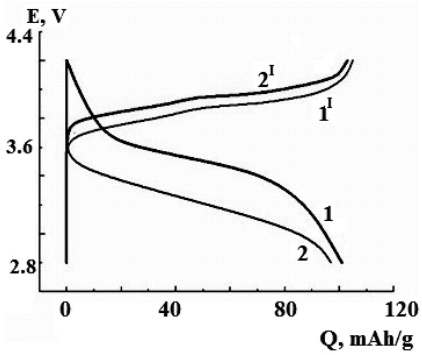

Fig. 6. The distinction between charge-discharge characteristics of $LiCo_{0.04}Mn_{1.96}O_4$–CNT electrodes obtained in three-electrode cell (curves 1, 1^I) and in two-electrode cell (curves 2, 2^I) at the charge rate of 1 C and the discharge rate of 10 C; the temperature is 258 K

Cyclic voltammetry studies on $LiCo_{0.04}Mn_{1.96}O_4$–CNT electrodes

Cyclic voltammograms (CV) of thin-layer composite $LiCo_{0.04}Mn_{1.96}O_4$–CNT electrodes show a reversible behavior of the system in three-electrode cell at the beginning of long cycling at temperature of 296 K. The difference between the cathodic and anodic peaks of the current ($dE=E_{cathode}-E_{anode}$) in two-phase reaction of the spinel composite with lithium (1) and (2) is insignificant (Fig. 7, curve 1). It is 18 mV for the redox couple at 4.05/4.00 V (site I) and 26 mV for the redox couple at 4.14/4.12 V (site II); the ratio of the cathodic capacity to the anodic one ($Q_{cathode}/Q_{anode}$) is 1.0 and 0.94 for the site I and (II), respectively. A significant kinetic deceleration appears in the system at a low temperature (Fig. 7, curve 2). The value of the difference, dE, grows and becomes as follows: dE=74 mV (site I), dE=84 mV (site II). The width of the semi-peaks also grows; the ratio $Q_{cathode}/Q_{anode}$ decreases to 0.84 and 0.78 for the site I and II, respectively. The both peak currents diminish, especially that at the potential of 4.14 V (site II).

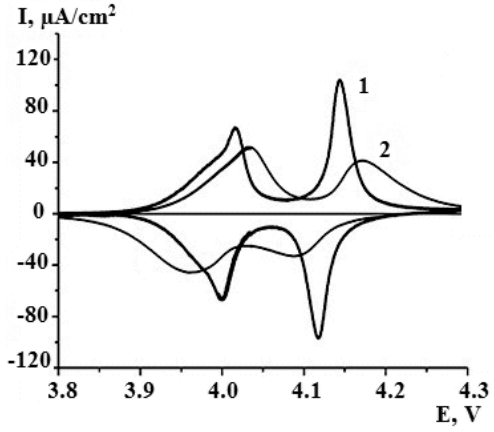

Fig. 7. Cyclic voltammograms of $LiCo_{0.04}Mn_{1.96}O_4$–CNT electrode at the following temperatures, K: 1 – 296; 2 – 258. The sweep rate is $1\cdot10^{-4}$ V·s^{-1}

The noticeable changes of the average

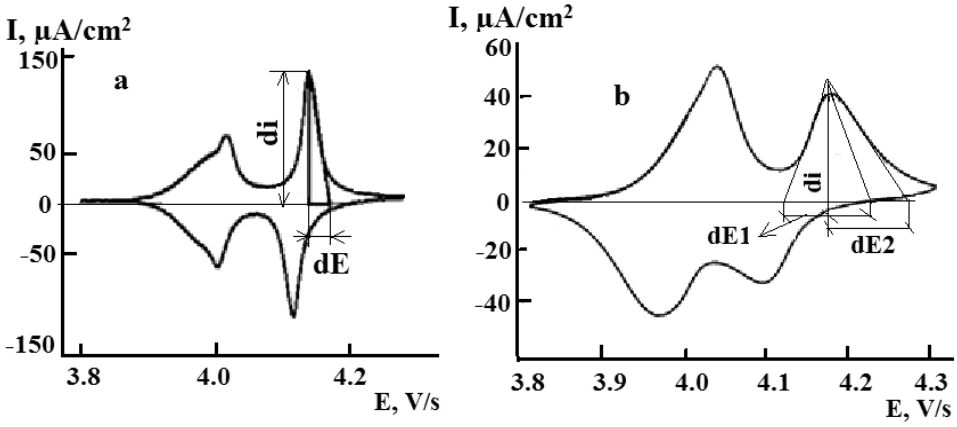

Fig.8. Determination of R_{CV}=dE/di from cyclic voltammograms of $LiCo_{0.04}Mn_{1.96}O_4$–CNT electrodes at the following temperatures, K: a – 296; b – 258

resistance, R_{CV}, occur at low temperatures. Here, the resistance, R_{CV}, is calculated as a ratio between the cathetus in CV-curve (R_{cv}=dE/di, Fig. 8,a, b). For the site II at the temperature of 296 K, the cathodic and anodic values of R_{CV} are $0.27 \cdot 10^3$ ohm·cm^2 and $0.28 \cdot 10^3$ ohm·cm^2, respectively.

The anodic CV-curve in site II is asymmetrical at the temperature of 258 K (Fig. 8,b). It may be separated into two components by the determination of its left-hand slope (obtained as $R_{CV1}=dE_1/di=1.69 \cdot 10^3$ ohm·cm^2) and the opposite-hand slope (obtained as $R_{CV2}=dE_2/di=3.50 \cdot 10^3$ ohm·cm^2). The difference between the obtained values ($R_{cv2}-R_{cv1}=dE_2/di-dE_1/di$) may be related to the resistance $R_{cv(side)}=1.81 \cdot 10^3$ ohm·cm^2. These data coincide well with the ratio of R_{sum}/R_{side} which was found in galvanostatic studies of the spinel composite.

The changes of the difference $dE_I=E_{anod\ peak}-E_{cathode\ peak}$ are not considerable when the discharge capacity of the spinel composite drops to 86 mA·h·g^{-1} on the 257th cycle at the temperature of 296 K as follows: dE_I=24 mV and dE_{II}=23 mV. The resistance R_{CV} grows as follows: $R_{CV}=0.48 \cdot 10^3$ ohm·cm^2 and $R_{CV}=0.40 \cdot 10^3$ ohm·cm^2 for the anodic and cathodic segments, respectively (Fig. 9, curve 1).

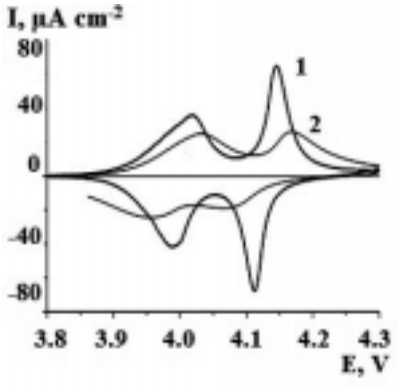

Fig. 9. Cyclic voltammograms of $LiCo_{0.04}Mn_{1.96}O_4$–CNT electrode recorded at the temperatures, K: 1 – 296 (257th cycle); 2 – 258 (256th cycle). The sweep rate is $1 \cdot 10^{-4}$ V·s^{-1}

The data presented after long cycling of the composite at the temperature of 258 K (Fig. 9, curve 2) differ from those at the temperature of 296 K (Fig. 9, curve 1). The parameters of the system change significantly at the 256th cycle. The discharge capacity drops to 74 mA·h·g^{-1}. The other parameters are as follows: dE_{II}=98 mV, dE_I=78 mV; the anodic $R_{CV}=2.68 \cdot 10^3$ ohm·cm^2, the cathodic $R_{CV}=3.20 \cdot 10^3$ ohm·cm^2; the width of semi-peaks grows, so it becomes difficult to be determined. It is clear that essential changes of dE and dR_{CV} parameters occur at low temperature. The peak current in site II decreases lower than that in site I. The capacity of composite electrode decreases more pronounced in site II, especially in two-electrode cell (Fig. 10).

Cyclic voltammograms were also obtained after long cycling (at the 183th cycle) at the temperature of 296 K (Fig. 11, curves 1, 2, 3). The linear dependence i_{peak} vs. $\omega^{1/2}$ in the range of sweep rate from 0.5 to $5.0 \cdot 10^{-4}$ V·s^{-1} evidences the diffusion control of intercalation/deintercalation processes.

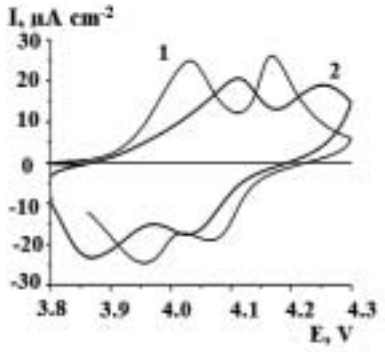

Fig. 10. Cyclic voltammograms of $LiCo_{0.04}Mn_{1.96}O_4$–CNT electrode recorded at the temperature of 258 K: 1 – 255th cycle in three-electrode cell; 2 – 256th cycle in two-electrode cell. The sweep rate is $1 \cdot 10^{-4}$ V·s^{-1}

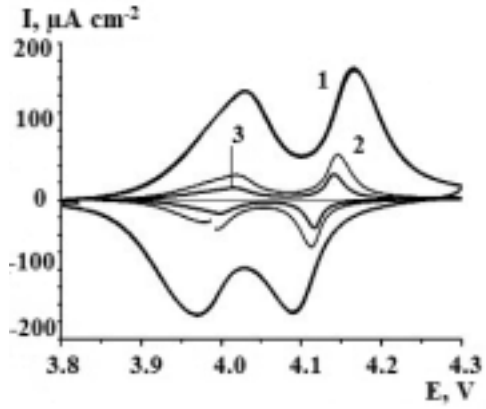

Fig. 11. Cyclic voltammograms of $LiCo_{0.04}Mn_{1.96}O_4$–CNT electrode recorded at different sweep rates, V·s^{-1}: 1 – $5 \cdot 10^{-4}$; 2 – $1 \cdot 10^{-4}$; 3 – $0.5 \cdot 10^{-4}$. The temperature is 296 K

Electrochemical impedance spectroscopy studies on $LiCo_{0.04}Mn_{1.96}O$–CNT electrode/electrolyte system

It was earlier shown [2] that the Nyquist plots of $LiCo_{0.04}Mn_{1.96}O_4$–CNT electrode/electrolyte system can be presented as two semicircles in their high- and middle-frequency parts and as a straight line at low frequencies in the frequency range of 10^5

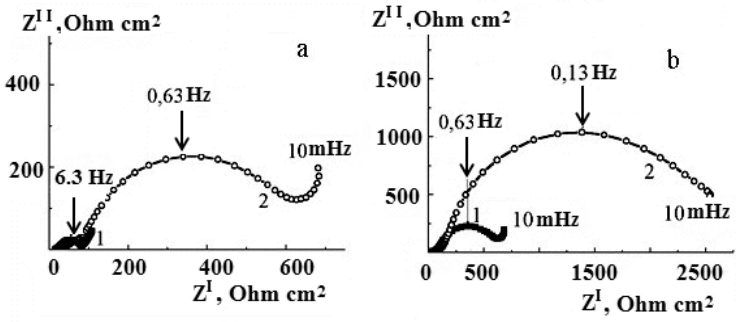

Fig. 12. Nyquist plots of composite $LiCo_{0.04}Mn_{1.96}O_4$–CNT electrode/electrolyte at the following temperatures, K: a – 296, b – 258. 1 – at the beginning of cycling, 2 – after long cycling

to 10^{-2} Hz; this is similar to studies of system $LiMn_2O_4$–CNT /electrolyte [1]. The parameters of EIS at maximal electrochemical activity of the composite on sites I and II in the redox reaction with lithium change when decreasing the temperature, these changes are more pronounced for the site II. Therefore, the data of galvanostatic and CV studies were analyzed in the work together with the data of EIS evolution in site II at the potential of 4.14 V.

The electrochemical impedance spectra of composite system at the temperatures of 296 K and 258 K are shown in Fig. 12,a, b. The discharge capacity at beginning of cycling is 117 mA·h·g^{-1} and 94 mA·h·g^{-1} at 296 and 258 K, respectively. The discharge capacity after long cycling is 93 mA·h·g^{-1} and 74 mA·h·g^{-1} at 296 and 258 K, respectively.

The semicircle in the high frequency region indicates Li^+-migration in a surface film of solid electrolyte interface (SEI). The semicircle in the middle frequency region implies the resistance of charge transfer through the interface of SEI film/composite R_{ct} shunted by electrical double-layer capacity of the composite C_{el}. The linear part of Nyquist plots characterizes the diffusion processes in the volume of the composite.

The effective exchange current, i_0, was calculated from the resistance of the charge transfer through SEI film/spinel composite interface, R_{ct}, by the measuring the diameter of the middle-frequency semicircle (Fig. 12,a, curve 1) using the known Buttler-Volmer equation for the 50th cycle at $Q_{discharge}$= =117 mA·h·g^{-1}. Its magnitude is $4.39 \cdot 10^{-4}$ A·cm^{-2} at the temperature of 296 K and it decreases 1.9 times when the discharge capacity decreases to 86 mA·h·g^{-1} at the 231th cycle, as estimated from R_{ct} value in Fig. 12,a, curve 2.

However, the changes of EIS are more marked at lower temperature (258 K) as it can be seen in Fig. 12,b, curve 1 for the 7th cycle. The resistance calculated from the EIS data increases by 3.0–3.5 times for SEI film (R_s) and by the order of the value for R_{ct}. Previous studies of Li-ion cells based on $LiMn_2O_4$ at sub-ambient temperatures revealed that the increase in cell impedance was generally due to the interfacial resistance of the cathode-electrolyte interface [7].

The value of i_0, determined from R_{ct} (Fig. 12,b, curve 2), decreases by the order of the value when the discharge capacity decreases to 74 mA·h·g^{-1} in the 270th cycle at the temperature of 258 K.

It should be noted that the inductive behavior or overlap periodically appears in the low frequency part of Nyquist plot near potential of 4.0 V vs. Li/Li^+-electrode at low temperature. Similar inductive behavior was previously detected for $LiMn_2O_4$ and attributed to an adsorption/desorption process of the electrolyte species [8]. Admittedly, it belongs to the side processes of the decomposition of the electrolyte. The decomposition of the electrolyte is accompanied by the formation of resistive surface film reflected by increased values of $R_{cv(side)}=(1.81–2.68) \cdot 10^3$ ohm·cm^2. The transformation of the surface film can be initiated by the adsorption/desorption process and the emergence of overlap tendency is its result.

The data of EIS, CV and galvanostatic investigations were compared. The effective exchange current, i_0, decreases at the potential of 4.16 V and the temperature of 258 K according to the EIS data. While peak of current decreases according to the CV data, the resistance of charge transfer, R_{ct}, increases according to the EIS data, and the resistance $dR_{galvan}=dE/di$ increases also as shown in galvanostatic studies.

An increase in R_{ct} resistance as well as in $dR_{galvan}=dE/di$ resistance in the galvanostatic studies of the composite thin films at the potentials not far from 4 V at T_{room} may be related to the anodic decomposition of the electrolyte. According to the

CV data, it is necessary to consider $R_{cv(side)}$ at low temperature for the elucidation of the causes for the discharge capacity drop of spinel composite.

The crucial role in the capacity decrease at low temperature belongs to the increase of the Li^+-migration resistance in electrolyte in the porous space of the spinel composite and the spinel composite resistances. The 3–4 times decrease of the electrolyte conductivity and the 6.5 times decrease of the spinel composite conductivity were shown at the temperature of 258 K. The structural adjustments of $LiMn_2O_4$ can be initiated when decreasing the temperature. The structure transition of cubic $LiMn_2O_4$ spinel symmetry (Fd3m) to orthorhombic symmetry (Fddd) with lattice parameters of a=8.2797 (2), b=8.244 (3), c=8.1198 (2) Å was shown to proceed at the temperature of 280 K [9]. Arrhenius slope of spinel composite under study in the temperature range of 272–307 K becomes broken at the temperature of 258 K. The charge-discharge characteristics of the composite $LiCo_{0.04}Mn_{1.96}O_4$–CNT electrodes are also broken at the temperature of 258 K.

The obtained results corroborate the conclusion about a narrow window of temperature stability of the used electrolyte (298–307 K), as was established in the study of thin-layer Mo_2S_3 electrodes by electrochemical impedance method [10]. We think that some ionic liquid, that allows the operation in 5 V Li batteries [11], may be an electrolyte with a wider window of electrochemical stability for the composite $LiCo_{0.04}Mn_{1.96}O_4$–CNT electrodes.

In our works [1,12], a positive effect on effective $LiMn_2O_4$ performance was shown in low-temperature mechanical composition of $LiMn_2O_4$–CNT that usually is accessible in high-temperature carbon $LiMn_2O_4$ composites [13]. The advantage of surface Co-doped $LiMn_2O_4$ were shown earlier over the volume Co-doped $LiMn_2O_4$ [14]. The efficiency of surface Co-doping of $LiMn_2O_4$ was affirmed in our works.

Conclusions

In this work, the discharge characteristics of $LiMn_2O_4$ spinel, which is generally used in Li-ion batteries, were investigated. We showed the improvement in cycling efficiency when using $LiMn_2O_4$ spinel in composition with CNT. The advantage of the proposed $LiCo_{0.04}Mn_{2-0.04}O_4$–CNT composite is its easy surface doping as compared with the volume doping. The $LiCo_{0.04}Mn_{2-0.04}O_4$–CNT composite shows high rate discharge characteristics and effective cycling ability at the ambient temperature (296 K). However, the high discharge characteristics of the composite decline at lower temperature (258 K). A special attention was paid to the low-temperature loss of the capacity of the composite $LiCo_{0.04}Mn_{1.96}O_4$–CNT electrodes and accumulator system on their basis during cycling. A decrease in the discharge electrode capacity is caused by decelerated electrode kinetics and increased iR-drop of voltage at low temperatures. The decrease of the capacity when cycling can be attributed to the loss of the electrode ability to full Li deintercalation and to the formation of the structural defects of $LiMn_2O_4$ spinel.

A decrease in the discharge characteristics of Co-doped $LiMn_2O_4$ spinel composition with CNT at low temperatures and long cycling is due to charge transfer through SEI film/spinel composite interface accompanied with diffusion of Li^+ ions in the bulk composite. The anodic decomposition of the electrolyte, which starts at 4.13 V vs. Li/Li^+-electrode, and the low conductivity of electrolyte containing EC, DMC, 1 mol L^{-1} $LiClO_4$ have a negative influence on the effective electrochemical performance of $LiCo_{0.04}Mn_{1.96}O_4$–CNT electrode/electrolyte/Li accumulator system at low temperature (258 K). The replacement of DMC by DME (dimetylether) in the electrolyte that was used in the work might increase the ionic conductivity at low temperature (253 K).

Acknowledgments

The current publication has been prepared in the framework of the project "Development the technology for fabrication of the high energy lithium batteries with polymer electrolyte" supported by Ministry of Education and Science of Ukraine (no. DZ/3-2016). The research supervisor of the project is Prof. E.M. Shembel.

REFERENCES

1. Apostolova R., Peskov R., Shembel E. Comparative performance of $LiMn_2O_4$ spinel compositions with carbon nanotubes and graphite in Li prototype battery. *Journal of Solid State Electrochemistry*, 2014, vol. 18, pp. 2315-2324.

2. Apostolova R., Peskov R., Shembel E. Compositions of Co-doped $LiMn_2O_4$ spinel with MCNT in lithium prototype accumulator. *ECS Transaction*, 2014, vol. 63, pp. 3-13.

3. Kovacheva D., Markovsky B., Salitra G., Talyosef Y., Gorova M., Levi E., Riboch M., Kim H.-J., Aurbach D. Electrochemical behavior of electrodes comprising micro- and nano-sized particles of $LiNi_{0.5}Mn_{1.5}O_4$: a comparative study. *Electrochimica Acta*, 2005, vol. 50, pp. 5553-5560.

4. Melezhik A.V., Sementsov Yu.I., Yanchenko V.V. Synthesis of porous carbon nanofibers on catalysts fabricated by the mechanochemical method. *Russian Journal of Applied*

Chemistry, 2005, vol. 78, pp. 924-930.

5. Aurbach D., Gamolsky K., Markovsky B., Salitra G., Gofer Y., Heider U., Oesten R., Schmidt M. The study of surface phenomena related to electrochemical lithium intercalation into Li_xMO_y host materials (M = Ni, Mn). *Journal of the Electrochemical Society*, 2000, vol. 147, pp. 1322-1331.

6. Striebel K.A., Sakai E., Cairns E.J. Impedance studies of the thin film $LiMn_2O_4$/electrolyte interface. *Journal of the Electrochemical Society*, 2002, vol. 149, pp. A61-A68.

7. Nagasubmanian G. Electrical characteristics of 18650 Li-ion cells at low temperatures. *Journal of Applied Electrochemistry*, 2001, vol. 31, pp. 99-104.

8. Pistoia G., Zane D., Zhang Y. Some aspects of $LiMn_2O_4$ electrochemistry in the 4 Volt range. *Journal of the Electrochemical Society*, 1995, vol. 142, pp. 2551-2557.

9. Oikawa K., Kamiyama T., Izumi F., Chakoumakos B.C., Ikuta H., Wakihara M., Li J., Matsui Y. Structure phase transition of the spinel–type oxide $LiMn_2O_4$. *Solid State Ionics*, 1998, vol. 109, pp. 35-41.

10. Kirsanova I.V., Apostolova R.D. Temperaturni efekty v systemi Mo_2S_3–elektrod/elektrolit Li akumulatora za danymy impedansnoiy spektroskopiy [Temperature effects in Mo_2S_3–electrode/ electrolyte of lithium battery system according to data of electrode impedance spectroscopy]. *Voprosi Khimii i Khimicheskoi Tekhnologii*, 2015, no. 5, pp. 17-21. (*in Ukrainian*).

11. Martha S.K., Markevich E., Burgel V., Salitra G., Zinigrad E., Markovsky B., Sclar H., Pramovich Z., Heik O., Aurbach D., Exnar I., Buqa H., Drezen T., Semrau G., Schmidt M., Kovacheva D., Saliyski N. A short review on surface chemical aspects of Li batteries: a key for a good performance. *Journal of Power Sources*, 2009, vol. 189, pp. 288-296.

12. Apostolova R. Thin-layer $LiMn_2O_4$, carbon nanotubes composite electrodes in lithium prototype accumulator. *ESC Transaction*, 2017, vol. 81, pp. 3-14.

13. Liu Q., Wang S., Tan H., Yang Z., Zeng J. Preparation and doping mode of doped $LiMn_2O_4$ for Li-ion batteries. *Energies*, 2013, vol. 6, pp. 1718-1730.

14. He X., Li J., Cai Y., Wang Y., Ying J., Jiang C., Wan C. Preparation of Co-doped spherical spinel $LiMn_2O_4$ cathode materials for Li-ion batteries. *Journal of Power Sources*, 2005, vol. 150, pp. 216-222.

Received 03.10.2017

ПІДВИЩЕННЯ ЕФЕКТИВНОСТІ ТОНКОШАРОВИХ ЕЛЕКТРОДІВ Co-ДОПОВАНА ШПІНЕЛЬ $LiMn_2O_4$–ВУГЛЕЦЕВІ НАНОТРУБКИ ДЛЯ ЗАСТОСУВАННЯ У Li-ІОННИХ БАТАРЕЯХ

Р.Д. Апостолова, Р.П. Пєсков

Проведено аналіз гальваностатичних кривих, циклічних вольтамперограм і імпедансних параметрів для визначення і пояснювання ключових факторів, які відповідні за зниження розрядних характеристик тонкошарових композитних електродів Co-допована шпінель $LiMn_2O_4$-вуглецеві нанотрубки в редокс-реакції з літієм у тривалому циклуванні при низькій температурі і підвищеній зарядно-розрядній швидкості. Проведено порівняння гальваностатичних кривих і циклічних вольтамперограм, одержаних в трьох- і дво-електродних експериментальних комірках; розглянуто також імпедансні спектри в залежності від температури і зарядно-розрядної швидкості. Це дозволило простежити еволюцію електродних процесів, які знижають розрядну ємкість, без застосування технічно складних і не завжди доступних методів дослідження. Ключову роль у зниженні розрядних характеристик композиції Co-допована шпінель з вуглецевими нанотрубками при низькій температурі і тривалому циклуванні відіграє перенесення зарядів через межу поверхнева твердо-електролітна плівка/шпінельний композит, ускладнений дифузією іонів Li^+ в об'ємі композиту. Установлено, що процеси анодного розкладання електроліту, які починаються при 4,13 В відносно Li/Li^+-електроду, і низька провідність електроліту ЕК, ДМК, 1 моль·л$^{-1}$ $LiClO_4$ при низькій температурі (258 К) негативно впливають на кулонівську ефективність перетворення акумуляторної системи $LiCo_{0.04}Mn_{1.96}O_4$–вуглецеві нанотрубки/електроліт/Li. У майбутньому одним із шляхів покращення електрохімічного перетворення указаної системи може бути оптимізація електроліту з застосуванням ефективних добавок. Зниження провідності шпінелі $LiMn_2O_4$ при низькій температурі (258 К) також призводить до зниження розрядної ємкості. Модифікація шпінельної композиції здається багатонадійною для стримування низько-температурних фазових переходів у шпінелі. Усування зазначених причин зниження розрядної ємкості у майбутньому полегшить реалізацію нового перспективного електродного матеріалу $LiCo_{0.04}Mn_{1.96}O_4$–вуглецеві нанотрубки у літій-іонному акумуляторі.

Ключові слова: літій-іонний акумулятор; Co-допована шпінель $LiMn_2O_4$–вуглецеві нанотрубки; падіння ємкості; гальваностатичні криві; циклічні вольтамперограми; імпедансні спектри.

INCREASING THE EFFICIENCY OF THIN-LAYER Co-DOPED $LiMn_2O_4$–CARBON NANOTUBES ELECTRODES FOR THE USE IN Li-ION BATTERIES

R.D. Apostolova, R.P. Peskov

Ukrainian State University of Chemical Technology, Dnipro, Ukraine

The analysis of galvanostatic curves, cyclic voltammograms and impedance parameters was performed in order to determine and interpret the key factors responsible for the decrease of the discharge characteristics of thin-layer composite Co-doped $LiMn_2O_4$ spinel–carbon nanotubes (CNT) electrodes in redox reaction with lithium during continuous cycling at low temperature and high charge-discharge rate. The comparison of galvanostatic curves and cyclic voltammograms obtained by using three-electrode and two-electrode experimental cells was carried out; the impedance spectra as functions of temperature and charge-discharge rate were considered too. This allowed following the evolution of degenerative electrode processes without the usage of research techniques which are complicated and not accessible enough. The charge transfer through the solid-electrolyte interface between solid-electrolyte film/spinel composite, complicated by diffusion of Li^+ ions in composite bulk, plays a key role in decreasing the discharge characteristics of Co-doped $LiMn_2O_4$ spinel composition with CNT at low temperatures and continuous cycling. It was established that the processes of anodic decomposition of the electrolyte starting at 4.13 V vs. Li/Li^+-electrode and low conductivity of electrolyte EC, DMC, 1 mol L^{-1} $LiClO_4$ at low temperatures (258 K) have a negative influence on the effective electrochemical performance of accumulator system $LiCo_{0.04}Mn_{1.96}O_4$, CNT-electrodes/electrolyte/Li. A further optimization of the electrolyte with the use of some efficient additions to the developed spinel composite can be a possible way to improve the electrode performance. A decrease in the conductivity of $LiMn_2O_4$ spinel results in a decrease in the capacity at low temperature (258 K). The modification of the spinel composite seems to be very promising to suppress its low-temperature phase transitions. The elimination of the established reasons for decreasing the capacity will facilitate the realization of new promising $LiCo_{0.04}Mn_{1.96}O_4$–CNT electrode material in lithium ion accumulators.

Keywords: lithium-ion accumulator; Co-doped $LiMn_2O_4$ spinel; carbon nanotubes; capacity; galvanostatic curves; cyclic voltammograms; impedance spectra.

REFERENCES

1. Apostolova R., Peskov R., Shembel E. Comparative performance of $LiMn_2O_4$ spinel compositions with carbon nanotubes and graphite in Li prototype battery. *Journal of Solid State Electrochemistry*, 2014, vol. 18, pp. 2315-2324.

2. Apostolova R., Peskov R., Shembel E. Compositions of Co-doped $LiMn_2O_4$ spinel with MCNT in lithium prototype accumulator. *ECS Transaction*, 2014, vol. 63, pp. 3-13.

3. Kovacheva D., Markovsky B., Salitra G., Talyosef Y., Gorova M., Levi E., Riboch M., Kim H.-J., Aurbach D. Electrochemical behavior of electrodes comprising micro- and nano-sized particles of $LiNi_{0.5}Mn_{1.5}O_4$: a comparative study. *Electrochimica Acta*, 2005, vol. 50, pp. 5553-5560.

4. Melezhik A.V., Sementsov Yu.I., Yanchenko V.V. Synthesis of porous carbon nanofibers on catalysts fabricated by the mechanochemical method. *Russian Journal of Applied Chemistry*, 2005, vol. 78, pp. 924-930.

5. Aurbach D., Gamolsky K., Markovsky B., Salitra G., Gofer Y., Heider U., Oesten R., Schmidt M. The study of surface phenomena related to electrochemical lithium intercalation into Li_xMO_y host materials (M = Ni, Mn). *Journal of the Electrochemical Society*, 2000, vol. 147, pp. 1322-1331.

6. Striebel K.A., Sakai E., Cairns E.J. Impedance studies of the thin film $LiMn_2O_4$/electrolyte interface. *Journal of the Electrochemical Society*, 2002, vol. 149, pp. A61-A68.

7. Nagasubmanian G. Electrical characteristics of 18650 Li-ion cells at low temperatures. *Journal of Applied Electrochemistry*, 2001, vol. 31, pp. 99-104.

8. Pistoia G., Zane D., Zhang Y. Some aspects of $LiMn_2O_4$ electrochemistry in the 4 Volt range. *Journal of the Electrochemical Society*, 1995, vol. 142, pp. 2551-2557.

9. Oikawa K., Kamiyama T., Izumi F., Chakoumakos B.C., Ikuta H., Wakihara M., Li J., Matsui Y. Structure phase transition of the spinel–type oxide $LiMn_2O_4$. *Solid State Ionics*, 1998, vol. 109, pp. 35-41.

10. Kirsanova I.V., Apostolova R.D. Temperaturni efekty v systemi Mo_2S_3–elektrod/elektrolit Li akumulatora za danymy impedansnoiy spektroskopiy [Temperature effects in Mo_2S_3–electrode/ electrolyte of lithium battery system according to data of electrode impedance spectroscopy]. *Voprosi Khimii i Khimicheskoi Tekhnologii*, 2015, no. 5, pp. 17-21. (*in Ukrainian*).

11. Martha S.K., Markevich E., Burgel V., Salitra G., Zinigrad E., Markovsky B., Sclar H., Pramovich Z., Heik O., Aurbach D., Exnar I., Buqa H., Drezen T., Semrau G., Schmidt M., Kovacheva D., Saliyski N. A short review on surface chemical aspects of Li batteries: a key for a good performance. *Journal of Power Sources*, 2009, vol. 189, pp. 288-296.

12. Apostolova R. Thin-layer $LiMn_2O_4$, carbon nanotubes composite electrodes in lithium prototype accumulator. *ESC Transaction*, 2017, vol. 81, pp. 3-14.

13. Liu Q., Wang S., Tan H., Yang Z., Zeng J. Preparation and doping mode of doped $LiMn_2O_4$ for Li-ion batteries. *Energies*, 2013, vol. 6, pp. 1718-1730.

14. He X., Li J., Cai Y., Wang Y., Ying J., Jiang C., Wan C. Preparation of Co-doped spherical spinel $LiMn_2O_4$ cathode materials for Li-ion batteries. *Journal of Power Sources*, 2005, vol. 150, pp. 216-222.